

Hyperspherical approach to a three-boson problem in two dimensions with a magnetic fieldSeth T. Rittenhouse,^{1,2} Andrew Wray,² and B. L. Johnson²¹*Department of Physics, The United States Naval Academy, Annapolis, Maryland 21402, USA*²*Department of Physics and Astronomy, Western Washington University, Bellingham, Washington 98225, USA*

(Received 16 November 2015; published 14 January 2016)

We examine a system of three-bosons confined to two dimensions in the presence of a perpendicular magnetic field within the framework of the adiabatic hyperspherical method. For the case of zero-range, regularized pseudopotential interactions, we find that the system is nearly separable in hyperspherical coordinates and that, away from a set of narrow avoided crossings, the full energy eigenspectrum as a function of the two-dimensional (2D) s -wave scattering length is well described by ignoring coupling between adiabatic hyperradial potentials. In the case of weak attractive or repulsive interactions, we find the lowest three-body energy states exhibit even-odd parity oscillations as a function of total internal 2D angular momentum and that for weak repulsive interactions, the universal lowest energy interacting state has an internal angular momentum of $M = 3$. With the inclusion of repulsive higher angular momentum we surmise that the origin of a set of “magic number” states (states with anomalously low energy) might emerge as the result of a combination of even-odd parity oscillations and the pattern of degeneracy in the noninteracting lowest Landau level states.

DOI: [10.1103/PhysRevA.93.012511](https://doi.org/10.1103/PhysRevA.93.012511)**I. INTRODUCTION**

The discovery of the fractional quantum Hall effect (FQHE) [1] provided an important impetus to investigate the physics of low-dimensional systems wherein particle-particle interactions play a fundamental role in the resulting dynamics. Since the original work of Laughlin [2], many theoretical approaches have been employed both to explain the observed collective behavior in the FQHE regime, and to expand the tools utilized for, and make connections between, a variety of strongly correlated many-body problems. In particular, model wave functions (building upon the original variational ground state proposed by Laughlin) have been employed to study the ground-state and elementary excitations [3,4], as well as composite-particle models [5–7], exact diagonalization for few-body systems [8–11], and special conformal field theories [12–14]. The problem is extremely rich; although much early work focused on interacting fermions, the generalization of the problem to other systems has been ongoing.

The richness associated with the fundamental dynamics of the FQHE regime [i.e., a system of two-dimensional (2D) charged particles under a large transverse dc magnetic field] may be traced to the dynamic bound states resulting from the interplay of the interparticle interactions and the external magnetic field. In 2D, any repulsive interaction will serve to separate the constituent particles to lower the energy, and the resulting separating motion will couple to the magnetic field, turning the particle trajectories back on themselves. The resulting dynamic many-particle bound state (in the absence of additional confining potentials) is a rich problem, even classically, wherein a primary feature is that the bound system is dominated by rotation, and thus the system angular momentum is a key feature [15–17]. A useful tool for connecting the classical problem to the quantum many-body problem is the study of the two-body FQH problem [18]; here, the problem is separable, and the precise role of the relative angular momentum is evident.

In the absence of interparticle interactions, the spectrum of a 2D charged gas under transverse field is comprised of a set

of highly degenerate Landau levels [19]. In the FQHE regime, the dynamic bound states described above are responsible for creating gaps in the energy spectrum *within* the Landau levels, and it is the origin and structure of these gaps, as well as the elementary excitations associated with them, that has garnered significant attention.

It was originally pointed out by Laughlin [20], and later studied in detail for few-body systems, that in the ground state of the interacting system in the lowest Landau level the angular momentum for small clusters goes up in integer multiples of the particle number [8]. In addition, exact diagonalization studies of few-body clusters interacting via Coulomb potentials exhibit “magic numbers” in ground-state energy of the system as a function of the total angular momentum [8,11]; at specific values of total angular momenta, local minima appear in the ground-state energy, and at specific values of the “magic” angular momenta, a corresponding maxima in the the excitation gap from the ground state appears [8]. The magic angular momenta for which the gaps appear are precisely those given by the trial ground-state wave function, and may be interpreted via the observation [11] that in the FQHE ground state, the relative angular momentum for each pair of particles is the *same*, and the total angular momentum is therefore found via $M = \sum m_{ij} = [N(N - 1)/2]q$, the usual result for the thermodynamic limit of large systems. Here, M is the total angular momentum, m_{ij} is the relative angular momentum quantum number for particles i and j , N is the total number of particles, and q is an odd integer (Fermi statistics). The origin of this remarkable result, and its dependence upon the form of the interactions, is an interesting question.

A further interesting question is whether or not the features of the FQHE regime generalize in a straightforward manner. In particular, can the structure of the vector potential and the particle interactions be projected in order to illuminate physical reasons for some of the fundamental structures? Recently, separation of the Schrödinger equation in hyperspherical coordinates in the FQHE regime demonstrated that the appearance of the FQHE may be associated with patterns in the degeneracy

of the states [21], a conjecture also made earlier by Stone *et al.* [10].

In this paper, we study the dynamics of few-body 2D bosonic systems interacting via regularized pseudopotential contact interactions under transverse magnetic field within the adiabatic hyperspherical method. The hyperspherical framework gives a convenient picture for studying the nature of the role of interactions and the degeneracy of the ground state, as well as the resulting Landau-level structure. When interactions are included, we find that, away from a set of narrow avoided crossings in the eigenspectrum, the three-boson problem is nearly separable in hyperspherical coordinates, in agreement with previous results for few electrons interacting via the Coulomb interaction [21]. Weak attractive or repulsive s -wave interactions also produce ground-state energies for fixed angular momentum that exhibit even-odd parity oscillations. On the repulsive side, we surmise that if repulsive higher angular momentum interactions are included, this parity oscillation combined with the degeneracy pattern of the lowest Landau level might be the source of the magic number behavior predicted in previous studies.

This paper is organized as follows. In Sec. II, we describe our theoretical approach including developing the Hamiltonian for three-bosons in 2D with a perpendicular magnetic field, separating out the center-of-mass motion, and transforming into hyperspherical coordinates. We also describe the Landau-level structure that results for the noninteracting case and develop a transcendental equation, the roots of which produce the adiabatic hyperradial potentials. In Sec. III, we examine the resulting adiabatic potentials and discuss the limiting cases of large and small s -wave two-body scattering length. In Sec. IV, the full eigenspectrum of the three-boson problem is presented as well as an analysis of the ground-state energy in the weakly repulsive and attractive limits. In Sec. V, the role of degeneracy is discussed as well as the part that degeneracy might play in the emergence of magic numbers in the three-boson system. Finally, in Sec. VI we summarize the results presented in the paper.

II. THEORETICAL METHODS

The few-body Hamiltonian that we are concerned with is that of three identical bosons confined to two dimensions in a vector potential appropriate to a constant effective magnetic field perpendicular to the plane of motion:

$$H = \sum_{i=1}^3 h_i + \sum_{i<j} V(r_{ij}), \quad (1)$$

$$h_i = \frac{1}{2m} (-i\hbar\nabla_i + \alpha\vec{A}_i)^2,$$

where h_i is the single-particle Hamiltonian for a particle moving in the vector potential \vec{A} , and $r_{ij} = |\vec{r}_i - \vec{r}_j|$ is the interparticle separation distance between particles i and j . Here, \vec{A}_i is the vector potential experienced by the i th particle, and α is an overall scaling factor. If the particles in question are charged particles, the scale factor would be simply given by $\alpha = q/c$ in Gaussian units. In Eq. (1), $V(r)$ is a pairwise isotropic interaction between two bosons that will be described more fully in the following. Since \vec{A} creates an effective

constant magnetic field, here we choose to describe this field in the symmetric gauge:

$$\vec{A} = \frac{B_0}{2} (\hat{x}y - \hat{y}x). \quad (2)$$

Note that we have chosen the magnetic field to be pointing in the $-z$ direction. Inserting the vector potential into Eq. (1) gives a total Hamiltonian in an illuminating form:

$$H = \sum_{i=1}^3 \left(\frac{-\hbar^2}{2m} \nabla_i^2 + \frac{1}{8} m \omega_c r_i^2 \right) - \frac{\omega_c}{2} L_{z, \text{Tot}} + \sum_{i<j} V(r_{ij}), \quad (3)$$

where $L_{z, \text{Tot}} = \sum_i \ell_{z,i}$ is the total angular momentum of the system. Here, we have written the Hamiltonian in terms of the cyclotron frequency $\omega_c = \alpha B/m$. The cyclotron frequency also yields a length scale $l_c = \sqrt{\hbar/m\omega_c} = \sqrt{\hbar/\alpha B}$ called the magnetic length. The utility of the symmetric gauge is now obvious: the effect of the magnetic field is simply that of an isotropic trap in the system along with an overall shift downward determined by the total angular momentum of the system.

To separate out the center of mass, we transform into a set of mass-scaled Jacobi coordinates [22,23]

$$\begin{aligned} \vec{\rho}_1^{(k)} &= \sqrt{\frac{\mu_{i,j}}{\mu}} (\vec{r}_i - \vec{r}_j), \\ \vec{\rho}_2^{(k)} &= \sqrt{\frac{\mu_{ij,k}}{\mu}} \left(\frac{\vec{r}_i + \vec{r}_j}{2} - \vec{r}_k \right), \\ \vec{R}_{\text{c.m.}} &= \frac{\vec{r}_1 + \vec{r}_2 + \vec{r}_3}{3}, \end{aligned} \quad (4)$$

where $\mu_{1,2} = m/2$ is the two-body reduced mass, $\mu_{ij,k} = 2m/3$ is the reduced mass of a two-body system with third particle, and μ is the three-body reduced mass which we choose to be $\mu = m/\sqrt{3}$. Here, the superscript (k) indicates which Jacobi coordinates have been chosen using the ‘‘odd-man out’’ notation where i, j, k is a cyclic permutation of the particle numbers, e.g., if $k = 3$ then $i = 1$ and $j = 2$. After the transformation, the total Hamiltonian can be written as

$$H = H_{\text{int}} + H_{\text{c.m.}}, \quad (5)$$

$$\begin{aligned} H_{\text{c.m.}} &= -\frac{\hbar^2}{2M_{\text{Tot}}} \nabla_{\text{c.m.}}^2 + \frac{1}{8} M_{\text{Tot}} \omega_c^2 R_{\text{c.m.}}^2 - \frac{\omega_c}{2} L_{\text{c.m., } z}, \\ H_{\text{int}} &= -\frac{\hbar^2}{2\mu} (\nabla_1^2 + \nabla_2^2) - \frac{\omega_c}{2} L_{\text{int}, z} \\ &\quad + \frac{1}{8} \mu \omega_c^2 (\rho_1^2 + \rho_2^2) + \sum_{i<j} V(r_{ij}). \end{aligned} \quad (6)$$

Here, $L_{\text{c.m., } z}$ is the angular momentum operator of the center of mass, $L_{\text{int}, z}$ is the internal angular momentum operator, and $M_{\text{Tot}} = 3m$ is the total mass of the three-body system. In Eq. (6), ∇_i refers to a derivative with respect to the i th Jacobi coordinate. It is important to point out that the internal Hamiltonian has the same form, independent of which Jacobi coordinate system has been chosen from Eq. (4) and thus the superscript (k) has been suppressed.

Since the center-of-mass motion is completely separated, we can proceed to examine the internal Hamiltonian H_{int} .

Because the interactions are isotropic, the total internal 2D angular momentum of the system is a good quantum number. If we restrict the system to only states with total internal angular momentum M , the Schrödinger equation that results from Eq. (6) is that of three particles confined to an isotropic oscillator with oscillator frequency $\omega_c/2$, i.e.,

$$E\Psi_M(\vec{\rho}_1^{(k)}, \vec{\rho}_2^{(k)}) = \left[\sum_i \left(\frac{-\hbar^2}{2\mu} \nabla_i^2 + \frac{1}{8} \mu \omega_c^2 \rho_i^2 \right) + \sum_{i < j} V(r_{ij}) - \frac{\omega_c}{2} M \right] \Psi_M(\vec{\rho}_1^{(k)}, \vec{\rho}_2^{(k)}), \quad (7)$$

where the first sum on the right-hand side runs over the Jacobi vectors. Here, $\Psi_M(\vec{\rho}_1^{(k)}, \vec{\rho}_2^{(k)})$ is a three-body eigenfunction with total internal angular momentum M .

A. Hyperspherical coordinates

To solve Eq. (7), we employ hyperspherical coordinates and the adiabatic hyperspherical representation, wherein the four-dimensional Schrödinger equation is expressed in terms of the hyperradius $R = \sqrt{\rho_1^2 + \rho_2^2}$ and a set of three hyperangles $\{\alpha, \phi_1, \phi_2\}$, collectively denoted by Ω , where ϕ_1 and ϕ_2 are the standard polar angles for Jacobi vectors $\vec{\rho}_1$ and $\vec{\rho}_2$, respectively, and α is an angle that correlates the lengths of the two Jacobi vectors, i.e.,

$$\begin{aligned} \rho_1 &= R \sin \alpha, \\ \rho_2 &= R \cos \alpha. \end{aligned}$$

In hyperspherical coordinates, the internal Hamiltonian of Eq. (6) can be written as

$$\begin{aligned} H_{\text{int}} &= \frac{-\hbar^2}{2\mu} \left(\frac{1}{R^2} \frac{\partial}{\partial R} R^3 \frac{\partial}{\partial R} - \frac{\Lambda^2}{R^2} \right) + \frac{i\hbar\omega_c}{2} \left(\frac{\partial}{\partial \phi_1} + \frac{\partial}{\partial \phi_2} \right) \\ &\quad + \frac{1}{8} \mu \omega_c^2 R^2 + \sum_{i < j} V(r_{ij}), \\ \Lambda^2 &= \frac{-1}{\sqrt{\sin \alpha \cos \alpha}} \frac{\partial^2}{\partial \alpha^2} \sqrt{\sin \alpha \cos \alpha} \\ &\quad - \frac{1}{\sin^2 \alpha} \left(\frac{\partial^2}{\partial \phi_1^2} - \frac{1}{4} \right) - \frac{1}{\cos^2 \alpha} \left(\frac{\partial^2}{\partial \phi_2^2} - \frac{1}{4} \right). \quad (8) \end{aligned}$$

Here, Λ^2 is the grand angular momentum operator, the properties and description of which can be found in a number of references (see Refs. [24–26] for example).

B. Landau levels

Before we solve the fully interacting system, it is instructive to consider the structure of the solutions to the noninteracting system of three particles in an external field. The quantized motion of a particle in an external field described in the symmetric gauge results in a set of infinitely degenerate levels called Landau levels, with energy spacing between degenerate manifolds of $\hbar\omega_c$. It is interesting to note that in setting the interactions in Eq. (8) to zero, the Hamiltonian becomes separable in hyperspherical coordinates, reproducing exactly the Landau-level picture, but with a slightly different

interpretation of the level structure. Here, excitations between Landau levels are achieved by either a hyperangular excitation in which the internal configuration of the bosons is changed, or through a hyperradial vibrational excitation in which the hyperradial motion is incremented as in a breathing mode.

The grand angular momentum operator is diagonalized using hyperspherical harmonics [24,25] with eigenvalues given by

$$\Lambda^2 Y_{\lambda m_1 m_2}(\Omega) = \lambda(\lambda + 2) Y_{\lambda m_1 m_2}(\Omega), \quad (9)$$

where λ is the grand angular momentum quantum number and m_1 and m_2 are the 2D angular momenta associated with the Jacobi vectors $\vec{\rho}_1$ and $\vec{\rho}_2$, respectively. Hyperspherical harmonics also diagonalize the total angular momentum of the system as

$$L_{z, \text{int}} Y_{\lambda m_1 m_2}(\Omega) = M Y_{\lambda m_1 m_2}(\Omega),$$

where $M = m_1 + m_2$ is the total 2D angular momentum of the system. The allowed values of λ are given by

$$\lambda = 2n + |m_1| + |m_2|, \quad (10)$$

where n is a non-negative integer. Note that λ has a minimum value given by $\lambda = |m_1| + |m_2|$ when $n = 0$.

Inserting the separability ansatz $\Psi(\vec{\rho}_1, \vec{\rho}_2) = \Psi(R, \Omega) = R^{3/2} F(R) Y_{\lambda m_1 m_2}(\Omega)$ into the Schrödinger equation resulting from Eq. (8) (with the interactions set to zero) results in a one-dimensional (1D) hyperradial Schrödinger equation of a harmonic oscillator with frequency $\omega_c/2$ that has been shifted down in energy by $M\hbar\omega_c/2$, i.e.,

$$\begin{aligned} 0 &= \left[\frac{-\hbar^2}{2\mu} \frac{\partial^2}{\partial R^2} + \frac{\hbar^2}{2\mu} \frac{(\lambda + 1/2)(\lambda + 3/2)}{R^2} \right. \\ &\quad \left. - \frac{\hbar\omega_c}{2} M + \frac{1}{8} \mu \omega_c^2 R^2 - E \right] F(R). \quad (11) \end{aligned}$$

Note that the $R^{3/2}$ factor in the separability ansatz is included to remove first derivatives in the hyperradius. This Schrödinger equation can be solved simply [27] with eigenenergies and eigenfunctions given by

$$E = \hbar\omega_c \left[\nu + \frac{(\lambda - M)}{2} + 1 \right], \quad \nu = 0, 1, 2, \dots \quad (12)$$

$$F(R) = A_{\nu\lambda} \frac{e^{-R^2/(2\sqrt{2}l_c)}}{R^{3/2}} \left(\frac{R}{\sqrt{2}l_c} \right)^{\lambda+3/2} L_{\nu}^{\lambda+1} \left(\frac{R^2}{2l_c^2} \right), \quad (13)$$

where l_c is the magnetic length, $L_{\nu}^L(x)$ is a Laguerre polynomial, and $A_{\nu\lambda}$ is a normalization constant. Inserting the restriction on values of λ from Eq. (10) into Eq. (12), the Landau-level picture emerges:

$$E = \hbar\omega_c \left(\nu + n + \frac{|m_1| + |m_2| - M}{2} + 1 \right). \quad (14)$$

Restricting ourselves to positive values of angular momentum, it is clear that for fixed ν and n any non-negative value of total angular momentum M produces the same energy, and thus an infinitely degenerate manifold of states. The structure of the energy levels seen in Eq. (14) is the same as the energy levels seen in the standard Landau-level picture. Here, however, the interpretation of excitation between Landau levels is

somewhat different. There are two different ways to move from one level to another, either through a hyperradial excitation by incrementing ν or through a hyperangular excitation by incrementing n .

C. Contact interactions and the adiabatic hyperspherical method

Next, we proceed to diagonalize the full interacting Hamiltonian of Eq. (8) within the adiabatic hyperspherical method. The heart of the approach is in treating the hyperradius R as an adiabatic parameter, and diagonalizing the Hamiltonian at fixed R in the remaining hyperangular degrees of freedom. In this method, the total wave function is expanded as

$$\Psi_M(\vec{\rho}_1, \vec{\rho}_2) = \sum_n R^{3/2} F_{nM}(R) \Phi_{nM}(R; \Omega). \quad (15)$$

Here, the adiabatic channel functions $\Phi_{nM}(R; \Omega)$ satisfy the fixed R Schrödinger equation

$$\left[\frac{-\hbar^2}{2\mu} \frac{\Delta^2}{R^2} + \sum_{i<j} V(r_{ij}) \right] \Phi_{nM}(\Omega) = u_{nM}(R) \Phi_{nM}(\Omega), \quad (16)$$

where $u_{nM}(R)$ is the adiabatic potential associated with $\Phi_{nM}(\Omega)$. Note that this is exactly the adiabatic Schrödinger equation that is solved in finding the adiabatic potentials for three bosons in the *absence* of any external field. Thus, $u_{nM}(R)$ are simply the adiabatic potentials for three interacting bosons confined to 2D, a system that has been studied extensively [28–33] and is of current interest in its own right. Inserting Eq. (8) and projecting onto the n th channel function results in a coupled system of one-dimensional Schrödinger equations in R :

$$E F_{nM}(R) = \left[\frac{-\hbar^2}{2\mu} \frac{d^2}{dR^2} + U_{nM}(R) - E \right] F_{nM}(R) - \frac{\hbar^2}{2\mu} \sum_{m \neq n} \left[\mathbf{Q}_{nm}(R) + 2\mathbf{P}_{nm}(R) \frac{d}{dR} \right] F_{mM}(R), \quad (17)$$

$$U_{nM}(R) = u_{nM}(R) + \frac{\hbar^2}{2\mu} \frac{3/4}{R^2} - \frac{\hbar^2}{2\mu} \mathbf{Q}_{nn}(R) + \frac{1}{8} \mu \omega_c^2 R^2 - \frac{\hbar \omega_c}{2} M. \quad (18)$$

Here, the effective hyperradial potentials are given by $U_n(R)$ and the nonadiabatic corrections embodied in the \mathbf{P} and \mathbf{Q} matrices are a result of hyperradial derivatives of the channel functions, i.e.,

$$\mathbf{P}_{nm} = \left\langle \left\langle \Phi_{nM}(R; \Omega) \left| \frac{\partial}{\partial R} \Phi_{mM}(R; \Omega) \right. \right\rangle \right\rangle, \quad (19)$$

$$\mathbf{Q}_{nm} = \left\langle \left\langle \Phi_{nM}(R; \Omega) \left| \frac{\partial^2}{\partial R^2} \Phi_{mM}(R; \Omega) \right. \right\rangle \right\rangle, \quad (20)$$

where the double brackets $\langle \langle \dots \rangle \rangle$ indicate that the matrix elements are taken over the hyperangular degrees of freedom only.

Up to this point, the treatment described above has been quite general, and is applicable to any two-body, cylindrically symmetric interaction. In fact, by extending the Jacobi coordinates to larger numbers of particles, this treatment can be extended to any N -body system. The adiabatic Schrödinger equation (16) has been solved for three-body systems with several different interaction potentials and can be approached by a number of different techniques [32–35]. In this work, we focus on the zero-range pseudopotential [36,37]

$$V(r) = \frac{\hbar^2}{m} \frac{\delta(r)}{r \left[1 - \ln\left(\frac{r}{a}\right) \right]} \frac{\partial}{\partial r} r, \quad (21)$$

where $a > 0$ is the 2D, s -wave ($m = 0$) scattering length. The effect of this pseudopotential is to enforce the two-body boundary condition

$$\lim_{r_{ij} \rightarrow 0} \frac{\partial}{\partial r_{ij}} \Phi_{nM}(R; \Omega) = C \left[1 + \frac{2 \tan \delta}{\pi} \left(\ln \frac{kr_{ij}}{2} + \gamma \right) \right],$$

$$\tan \delta = \frac{\pi}{2 \left(\ln \frac{ka}{2} + \gamma \right)}, \quad (22)$$

where C is a constant, δ is the 2D s -wave scattering phase shift, k is the two-body wave number, and $\gamma = 0.5772$ is the Euler constant. It is important to note that this pseudopotential only affects wave functions with an s -wave component of the angular momentum between pairs of particles; all higher partial waves are treated as noninteracting. This pseudopotential is accurate in the low-energy limit when the true interparticle interaction falls off sufficiently fast at large r to be considered short range. We also require that both the range r_0 and the effective range r_{eff} of the interaction are the smallest length scales in the system, i.e., $a \gg r_0, r_{\text{eff}}$ and $l_c \gg r_0, r_{\text{eff}}$. At the two-body level, this pseudopotential interaction produces a large halo dimer state with binding energy $E_b = -4e^{-2\gamma}/ma^2$ [37]. It is also worth noting that in the limit of large or small scattering length $ka \rightarrow \infty$ or $ka \rightarrow 0$, where k is the relative two-body momentum, the pseudopotential approaches the noninteracting limit.

In this study, we employ the hyperangular Green's function approach of Ref. [38]. The full derivation using this method is somewhat tedious, but straightforward, and we will not detail it here. The heart of the method is in turning the adiabatic Schrödinger equation into a Lippmann-Schwinger (LS) equation by employing the free-space hyperangular Green's function. Within this LS equation, it is easy to apply the boundary condition of Eq. (22) when two particles are in contact with each other, and propagate the particles freely between such contact points. The result of this derivation gives the adiabatic potentials as

$$u_{nM}(R) = \frac{\hbar^2}{2\mu} \frac{\varepsilon_{nM}(R) - 1}{R^2}, \quad (23)$$

where we refer to $\varepsilon_{nM}(R)$ as the hyperangular eigenvalues which are roots of the transcendental equation

$$-\ln \frac{R}{a} = \ln \sqrt{\frac{2\mu}{m}} - \gamma - \frac{1}{2} \psi \left(\frac{M - \sqrt{\varepsilon_{nM}} + 1}{2} \right) - \frac{1}{2} \psi \left(\frac{M + \sqrt{\varepsilon_{nM}} + 1}{2} \right)$$

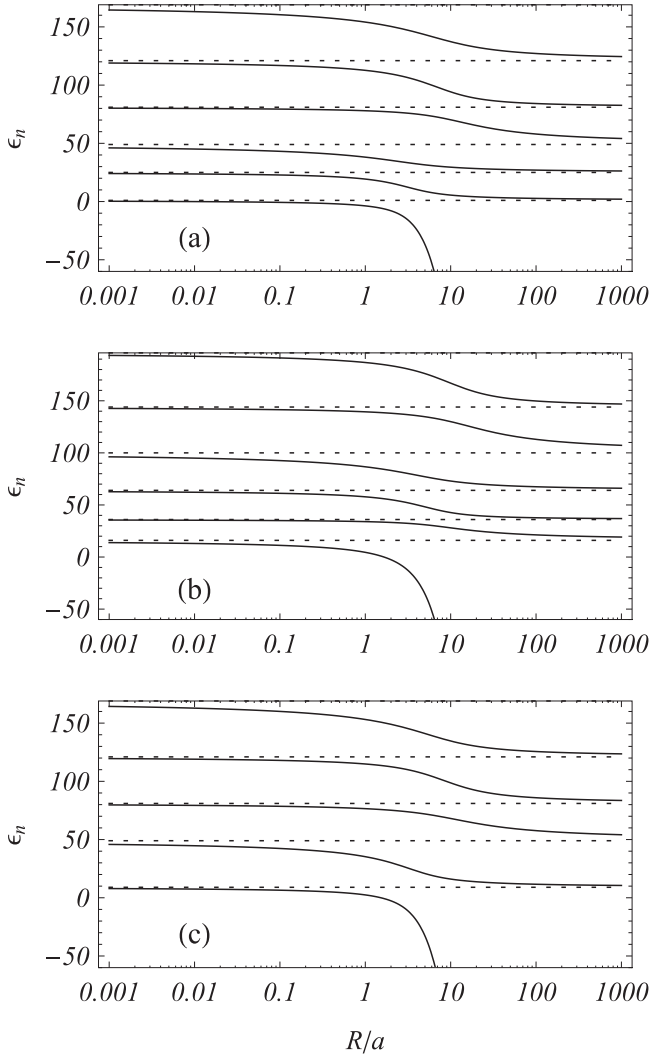


FIG. 1. The first several adiabatic hyperangular eigenvalues for angular momentum (a) $M = 0$, (b) $M = 1$, and (c) $M = 3$ are shown as a function of R/a on a log scale. Dotted lines indicate the hyperangular eigenvalues of hyperspherical harmonics of noninteracting systems expected in the large- and small- a limits.

$$\begin{aligned}
 & + \left(\frac{-1}{2}\right)^M \frac{\Gamma\left(\frac{M+\sqrt{\varepsilon_{nM}+1}}{2}\right)\Gamma\left(\frac{M-\sqrt{\varepsilon_{nM}+1}}{2}\right)}{\Gamma(M+1)} {}_2F_1 \\
 & \times \left(\frac{M-\sqrt{\varepsilon_{nM}+1}}{2}, \frac{M+\sqrt{\varepsilon_{nM}+1}}{2}; M+1; \frac{1}{4}\right),
 \end{aligned} \quad (24)$$

where $\Gamma(x)$ is the gamma function, $\psi(x) = \Gamma'(x)/\Gamma(x)$ is the digamma function, and ${}_2F_1(a, b; c; x)$ is a hypergeometric function. In the case where $M = 0$, this reduces to the results found in Refs. [28,32].

Examples of the hyperradial eigenvalues ε_{nM} for $M = 0, 1$, and 3 are shown in Fig. 1 as a function of R/a . In each case, the lowest hyperangular eigenvalue goes to $-\infty$ quadratically in R in the large- R limit. This corresponds to a particle-dimer hyperangular channel function consisting of a free particle far away from a bound dimer. With the exception of the lowest potential in the large- R limit, all

hyperangular eigenvalues logarithmically approach an integer, corresponding to a noninteracting value, in both the large- and small- R limits. The hyperangular eigenvalues transition from one noninteracting limit to another in the region where $R \sim a$.

We can understand this behavior by considering the pseudopotential in Eq. (21). In the limit of large hyperradius $R \gg a$, the average interparticle separation is much greater than the scattering length $r \gg a$. The logarithmic behavior of the scattering length in the pseudopotential indicates that this is a weakly repulsive limit. In the limit of very small hyperradius $R \ll a$, the average interparticle separation is much smaller than the scattering length $r \ll a$, again, because of the logarithmic nature of the pseudopotential, this becomes the weakly attractive limit.

The matrix elements of the nonadiabatic correction matrix \mathbf{P} [Eq. (19)] are given in Ref. [32] in terms of the hyperangular eigenvalues by

$$\mathbf{P}_{mn} = \frac{\sqrt{\varepsilon'_{mM}(R)\varepsilon'_{nM}(R)}}{\varepsilon_{mM}(R) - \varepsilon_{nM}(R)}, \quad (25)$$

where the primes indicate a derivative with respect to R . The diagonal correction $\mathbf{Q}_{nn}(R)$ to the potentials in Eq. (18) is given by

$$\mathbf{Q}_{nn} = -\frac{1}{12R^2} - \frac{1}{4} \left[\frac{\varepsilon''_{nM}(R)}{\varepsilon'_{nM}(R)} \right]^2 + \frac{\varepsilon'''_{nM}(R)}{6\varepsilon'_{nM}(R)}. \quad (26)$$

In the infinite channel limit, the off-diagonal elements of \mathbf{Q} can be found using the identity

$$\mathbf{Q}_{mn} = \mathbf{P}'_{mn}(R) + [\mathbf{P}^2]_{mn}, \quad (27)$$

where $[\mathbf{P}^2]_{mn}$ is the mn th element of the square of the \mathbf{P} matrix and \mathbf{P}' indicates a derivative with respect to the hyperradius. While Eq. (27) is only exact in the infinite channel limit, for the purposes of this work, we will use it in a finite channel number expansion to approximate direct, off-diagonal, nonadiabatic contributions.

III. ADIABATIC POTENTIALS

One of the strengths of the adiabatic hyperspherical method is that, with the effective adiabatic potentials in hand, we can bring all of the understanding and intuition of normal 1D Schrödinger quantum mechanics to bear on the problem. The adiabatic potentials of Eq. (18) can give significant insight into the structure and behavior of the three-body system. Figure 2(a) shows the lowest three potentials for total angular momentum $M = 0$ for scattering lengths $a = 0.1l_c$, $a = 7l_c$, and $a = 10000l_c$. Figure 2(b) shows the same for a system with total angular momentum $M = 2$. The insets in Figs. 2(a) and 2(b) show the potentials for $a = 10000l_c$ over a larger range of R to illustrate the effective oscillator potential that is introduced as a consequence of the magnetic field. In the adiabatic potentials, there is a competition between two length scales: the scattering length a , which controls the interactions, and the magnetic length l_c , which is controlled by the magnetic field. In the small- a limit, the minimum of lowest adiabatic potential is shifted down far below the zero-energy threshold. In fact, in the absence of any field this potential asymptotically goes to an energy of $U \rightarrow -4 \exp(-2\gamma)\hbar^2/ma^2$ which is

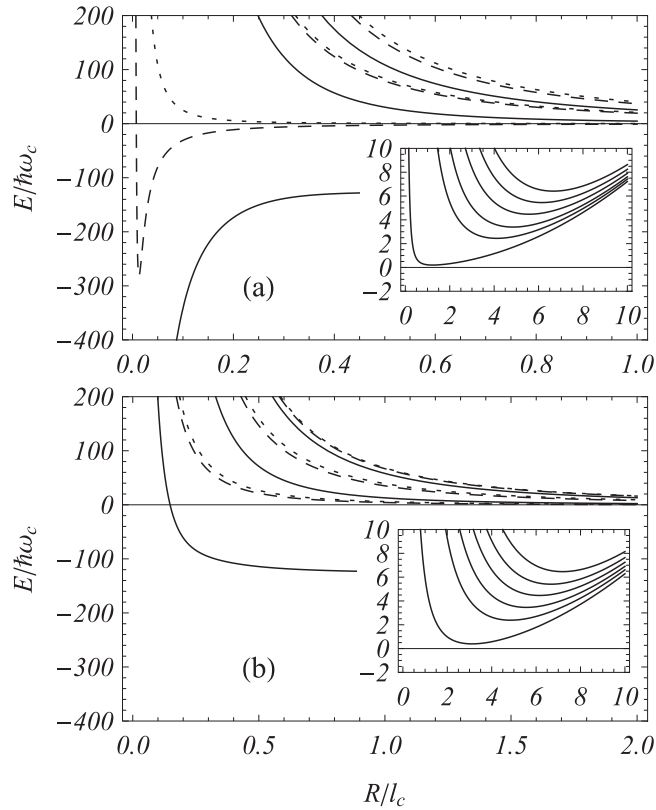


FIG. 2. The lowest three adiabatic potentials are shown for $M = 0$ (a) and $M = 2$ (b) as a function of R in units of the magnetic length l_c for several different values of the scattering length $a = 0.1l_c$ (solid curves), $a = 7l_c$ (dashed curves), and $a = 10000l_c$ (dotted curves). (Insets) The lowest three adiabatic potentials for $a = 10000l_c$ are shown over a different scale to illustrate the effective oscillator potential imposed by the external magnetic field.

exactly the energy of the dimer state. As a result, we can interpret the lowest potential in the small scattering length limit as describing an effective two-body interaction potential of a particle and an $m = 0$ dimer in a weak external field, a behavior that persists for all values of M .

In the small scattering length limit the second adiabatic potential is similar to a harmonic oscillator potential, and in the absence of any magnetic field asymptotes to the zero-energy threshold. This allows us to interpret the lowest adiabatic interaction channel as that corresponding to the behavior of a three-body system with no dimer-type bound states. Another feature that can be seen in the lowest $M = 0$ adiabatic potential is a short-range attractive well that is not present for any other values of M . For small a , this well is deep enough to bind two three-body states with binding energies of $E = 16.25E_b$ and $1.26E_b$, respectively, where E_b is the dimer binding energy. These values are found using a single-channel calculation and are in good agreement with three-body bound-state energies in the absence of the magnetic field found in Refs. [32,39].

In the large scattering length limit $a \gg l_c$, the hyperangular eigenvalues are dominated by the small hyperradius behavior, meaning that the potentials are close to the noninteracting limit. In this limit, the particles are all kept close together by the (strong) external field and the average interparticle separation

is much smaller than the scattering length. This means that any particle-dimer-type behavior is pushed to the large- R regime energetically far removed from the minimum. Thus, all of the potentials can be considered to correspond with true three-body behavior.

In general, when the hyperradius is much larger than the scattering length $R \gg a$, the three-body potentials (those not associated with particle-dimer-type behavior) approach the noninteracting limit. When the scattering length is much smaller than the magnetic length, the minimum in the harmonic potential resides at $R \sim l_c \gg a$ and deviations from the noninteracting behavior are energetically inaccessible. Therefore, we can expect the system to approximately behave as three noninteracting particles in an external field. For the lowest potential, associated with particle-dimer behavior, with the exception of the $M = 0$ states, we can expect that the system will behave as a noninteracting two-body system in an external field whose ground-state energy is shifted by the dimer binding energy. For $M = 0$, the deep well in the $R < a$ region in the potentials will modify this behavior.

In the $R \ll a$ limit, all of the potentials have noninteracting limiting behavior. When the scattering length is much smaller than the magnetic length, any changes in the potentials that result from the interaction are in the small hyperradius region, pushed far up the inner potential barrier that can be seen in the inset of Figs. 2(a) and 2(b). We can therefore expect that the behavior of the system will again approach that of the noninteracting system in the $a \gg l_c$ limit. With the potentials in hand, we can now examine the eigenspectrum of the system.

IV. THREE-BODY ENERGIES

In this section, we describe the behavior of the eigenspectrum that results from the coupled system of 1D Schrödinger equations from Eq. (17). Generally, it is necessary to include many adiabatic channels to converge the bound-state energies of three bodies in two dimensions to high accuracy; however, to achieve accuracy to within several digits, only relatively few channels are needed. With that in mind, we solve Eq. (17) using the lowest six adiabatic channels for each total angular momentum M . We have found that this is sufficient to converge the energetically low-lying states to within $\sim 0.1\%$ accuracy, which is sufficient for the purposes of this study.

The full eigenspectrum of the three-boson system for $M = 0, 1$, and 2 including the off-diagonal couplings between adiabatic channels is shown as a function of a/l_c in red in Figs. 3(a)–3(c). Also shown in Figs. 3(a)–3(c) are the energies of the lowest six hyperradial vibrational states for each effective potential $U_{nM}(R)$, ignoring the off-diagonal coupling matrices \mathbf{P} and \mathbf{Q} but including the diagonal correction $\mathbf{Q}_{nm}(R)$. In regions nearby crossings between uncoupled energies, the off-diagonal couplings $\mathbf{P}_{nm}(R)$ and $\mathbf{Q}_{nm}(R)$ introduce a series of narrow avoided crossings in the energy spectrum as a function of the scattering length and these off-diagonal direct and derivative couplings become important in these areas. However, away from these avoided crossings, the uncoupled adiabatic potentials $U_{nM}(R)$ provide a good approximation of the energy spectrum of the three-particle system indicating that the system is nearly separable within the adiabatic hyperspherical framework which provides an accurate description of this

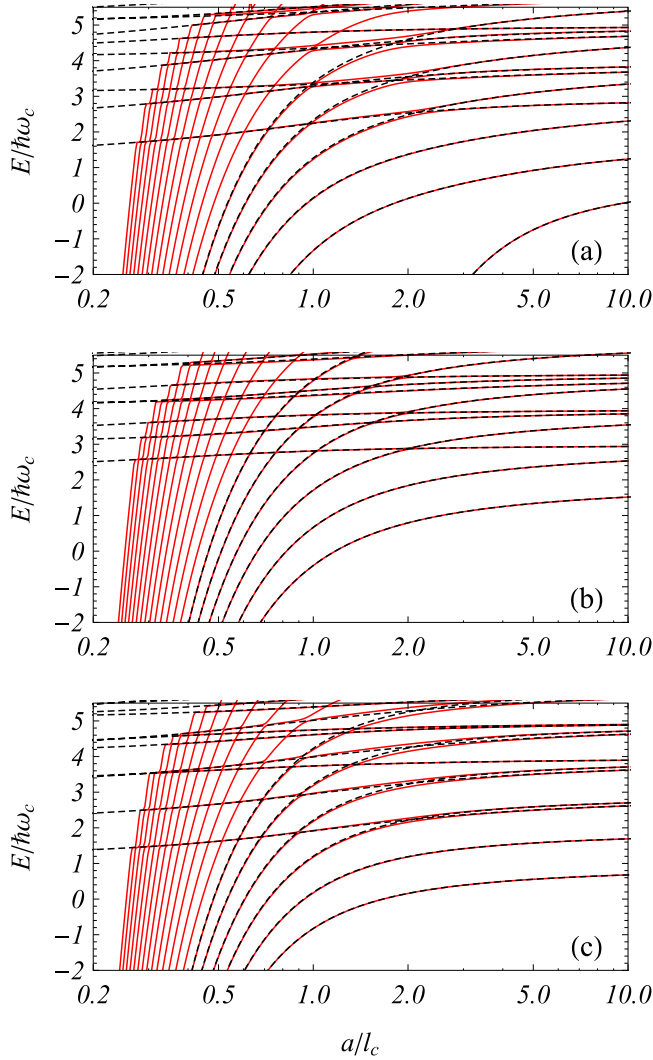


FIG. 3. The full energy spectrum in units of $\hbar\omega_c$ is shown as a function of a/l_c . The energies were calculated for total angular momentum $M = 0$ (a), $M = 1$ (b), and $M = 2$ (c) including (solid red line) and ignoring (dashed black line) couplings between adiabatic channels.

system. As a result, unless otherwise stated, we will focus on the uncoupled adiabatic channel energies for the remainder of this paper.

Figures 4(a)–4(c) show the vibrational energies for the lowest three adiabatic channels as a function of a/l_c for $M = 0, 1$, and 2 , respectively. In each case, the lowest adiabatic channel has vibrational states that decrease in energy as $1/a^2$ for $a \ll l_c$. These are states associated with an atom-dimer interaction channel. For $M = 0$, the lowest two vibrational states in the lowest channel become the three-body bound state mentioned previously. While atom-dimer states are of interest in their own right, we are interested here in the behavior of three-body states in the presence of an external field, and the atom-dimer states in the small scattering length limit will not be the focus of this work. For the second and third adiabatic channels, we can see that at very small scattering lengths, the three-body energies approach the noninteracting Landau-level values as expected. In sweeping from small to large scattering

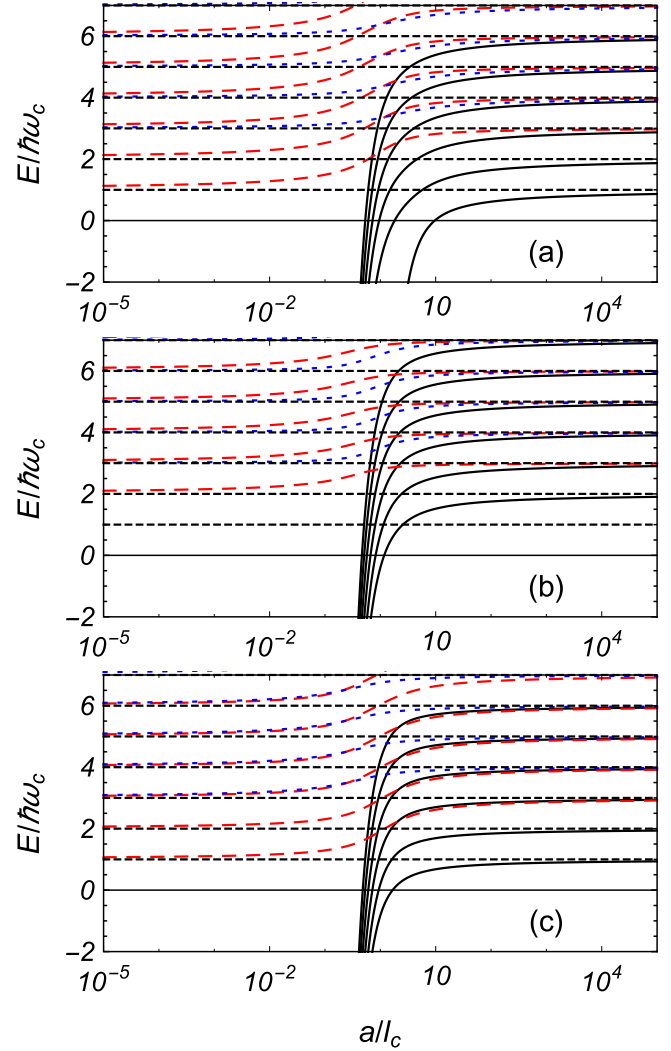


FIG. 4. The energies of the first six vibrational levels attached to the first (solid black curves), second (dashed red curves), and third (dotted blue curves) adiabatic channels are shown as a function of scattering length for internal angular momentum (a) $M = 0$, (b) $M = 1$, and (c) $M = 2$. The coupling between adiabatic channels has been ignored here. The Landau-level energies are shown as black dashed lines for reference.

length, the energies transition up smoothly to a higher Landau level in the large scattering length limit. In the small- a limit, the energies are shifted up slightly from the noninteracting energy corresponding to an effectively repulsive interaction. The energies of the system in the large scattering length limit are shifted slightly down from the noninteracting Landau levels corresponding to an effectively attractive interaction.

In the large and small scattering length limits, Fig. 4(b) shows that the lowest $M = 1$ adiabatic channel that corresponds to a three-body state converges to the second Landau level rather than the first. As discussed later, this is because a total internal angular momentum of $M = 1$ in the lowest Landau level is forbidden for bosonic symmetry and the lowest noninteracting three-boson state with internal angular momentum $M = 1$ corresponds to the second Landau level.

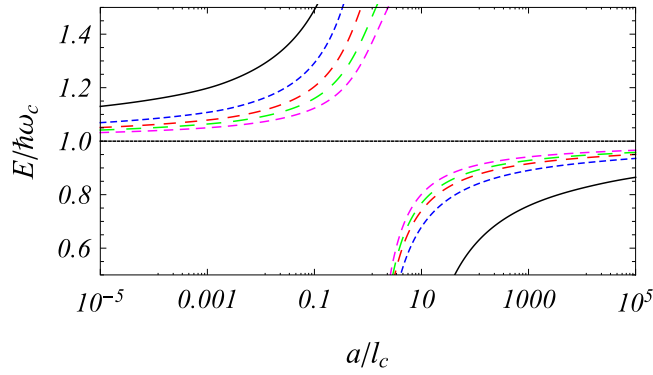


FIG. 5. The lowest vibrational state energy for each adiabatic channel is shown for $M = 0, 2, 3, 4,$ and 5 as a function of a/l_c on a log scale. The energies for $M = 0$ are shown as solid curves while the energies for $M = 2-5$ are shown as dashed curves with increasing dash size for increasing values of M . The noninteracting Landau level is shown for reference.

Of particular interest here is the behavior of the lowest-energy three-body state. Figure 5 shows the energy of the lowest three-body state for $M = 0, 2, 3, 4,$ and 5 (shown in black, blue, magenta, red, and green, respectively) as a function of a/l_c in the region near the lowest Landau level. Because there are no $M = 1$ lowest Landau-level states, $M = 1$ is excluded here. There are several interesting things that can be observed in this figure. First, we can see that at small scattering length $a < l_c$, the three-body energies are pushed above the lowest Landau level indicating that this interaction regime corresponds to repulsive interactions. For large scattering length $a > l_c$, the three-body energies are below the lowest Landau level indicating that this is the attractive interaction regime. We also note that for $M \geq 2$ the levels show a parity oscillation, with M even higher in energy for small scattering length and M odd lower in energy, and vice versa in the large scattering length limit.

The opposite parity oscillation is shown in Fig. 6 in which we have plotted the lowest-energy three-body state versus internal angular momentum M for small scattering length [$a = 0.1l_c$ in Fig. 6(a)] and large scattering length [$a = 100l_c$ in Fig. 6(b)]. This parity oscillation can be understood simply by understanding that even parity states (even M) tend to have the three bosons in closer proximity and thus more strongly feel the s -wave contact interactions than the odd-parity (odd- M) states. It is interesting to note here that because $M = 1$ is forbidden for bosonic symmetry in the lowest Landau level, $M = 3$ is *universally* the lowest-energy three-body state for states interacting via repulsive, $a < l_c$, s -wave contact interactions.

At larger angular momentum, we would expect an angular momentum (centrifugal) barrier to form that prevents the bosons from being near each other. Thus, we might expect that the energy should tend towards the noninteracting value of the lowest Landau level. This behavior is not borne out in Fig. 6, where we observe that the energies of the three-boson states tend towards a constant that is above the lowest Landau level for repulsive interactions and below it when the interactions are attractive. The explanation for this apparent inconsistency

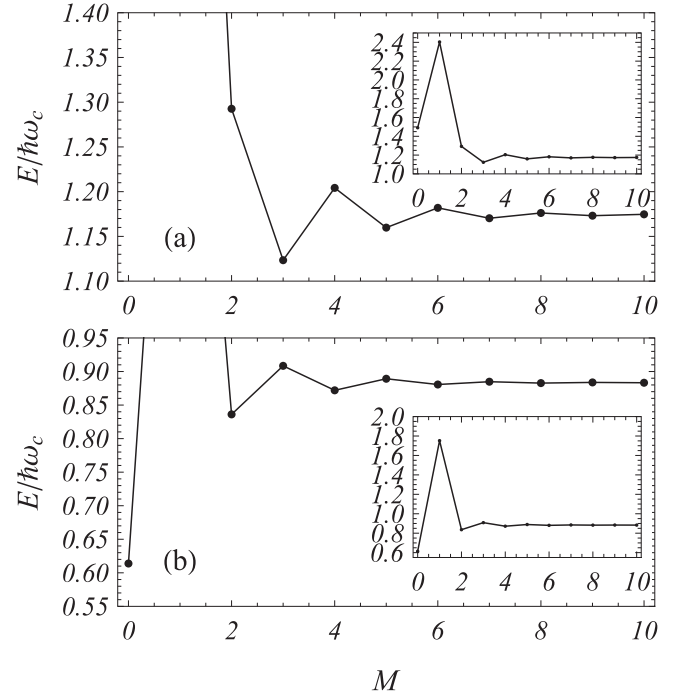


FIG. 6. The energy of the lowest three-body state (the state without any dimerlike characteristics) is shown as a function of internal angular momentum M for (a) the weakly repulsive ($a = 0.1l_c$) and (b) weakly attractive ($a = 100l_c$) regimes. Note that for $M > 1$ the energies oscillate with parity with odd M being lower in energy for small scattering length and even M being lower for large scattering length. Universally for small scattering length, the lowest $M = 3$ state is the lowest interacting three-body state for small a/l_c . (Insets) Show the same states on a larger scale to include the lowest $M = 1$ state.

lies in the regularized s -wave contact interaction of Eq. (21). This interaction projects onto only those states which have some component of their wave functions with zero interparticle angular momentum. Examining the energy-level structure of the lowest Landau level from Eq. (14) with $m_1 = 0$, we can see that for each value of total internal angular momentum, there is at most one such lowest Landau level state. When the lowest Landau level for a given value of M is degenerate, there will be additional states in which the interparticle angular momentum has no $m = 0$ component and will be noninteracting according to our pseudopotential.

V. ROLE OF DEGENERACY

Recently, Daily *et al.* [21] have highlighted the crucial role that the degeneracy of the lowest Landau level plays in the energetic structure of 2D few-fermion systems interacting via the Coulomb potential in the presence of an external magnetic field. This degeneracy plays an equally important role in this study. As mentioned above, at most only a single lowest Landau level state for each internal angular momentum value M has a zero interparticle angular momentum component in the three-boson system. However, as the value of M increases, the degeneracy generally increases as well. A complete description of the degeneracy of the lowest Landau

level for N identical fermions (which can be directly applied to N identical bosons) is given in Ref. [21]; we will briefly reiterate the argument here for completeness.

The noninteracting N -body Hamiltonian from Eq. (1), with $V(r) = 0$, is separable in individual particle coordinates where the bosonic lowest Landau level wave functions are given by

$$\Psi_{\text{LL}} = \mathcal{N} \hat{\mathbf{S}} \prod_{j=1}^N z_j^{m_j} e^{-|z_j|^2/l_c^2}, \quad (28)$$

where $z_j = x_j + iy_j$ is the j th boson's position in the laboratory frame written in complex coordinates and $m_j \geq 0$ is the angular momentum of particle j . Here, $\hat{\mathbf{S}}$ is a symmetrization operator that imposes bosonic symmetry and \mathcal{N} is a normalization factor. In the symmetrized basis, the individual angular momenta are no longer good quantum numbers; however, the total angular momentum $M_{\text{Tot}} = \sum_{j=1}^N m_j$ is conserved. Using this, the degeneracy of the lowest Landau level is given by the number of ways we can combine N individual particle angular momenta to get M_{Tot} subject to the condition that $m_1 \leq m_2 \leq m_3 \dots$ so that we do not double count any symmetric configurations. This means that the degeneracy $D_{\text{Tot}}(M_{\text{Tot}})$ for total angular momentum M_{Tot} for N particles is given by the number of integer partitions P_N of no more than N integers of M_{Tot} , i.e., $D_{\text{Tot}} = P_N(M_{\text{Tot}})$ where we define $P_N(0) \equiv 1$.

The noninteracting Hamiltonian is also separable into internal and center-of-mass degrees of freedom as seen in Eq. (5). In this basis, the total angular momentum can be written in terms of the internal angular momentum M and the center-of-mass angular momentum $M_{\text{c.m.}}$ as $M_{\text{Tot}} = M + M_{\text{c.m.}}$. The degeneracy of the lowest Landau level for internal angular momentum M , $D(M)$, is given by the degeneracy when the total angular momentum is entirely internal, i.e. $M_{\text{Tot}} = M$ and $M_{\text{c.m.}} = 0$. However, the degeneracy $D_{\text{Tot}}(M_{\text{Tot}})$ from above includes all allowed values of the center-of-mass angular momentum $0 \leq M_{\text{c.m.}} \leq M_{\text{Tot}}$. To find only the degeneracy of the states with $M_{\text{c.m.}} = 0$, we must subtract off the total number of configurations with $M_{\text{c.m.}} = 1, 2, 3, \dots, M$. Because each center-of-mass angular momentum is nondegenerate, and the fact that for each value of M there is only one value of $M_{\text{c.m.}}$ that gives $M_{\text{Tot}} = M + M_{\text{c.m.}}$, the number of states with $M_{\text{c.m.}} = 1, 2, 3, \dots, M$ with $M_{\text{Tot}} = M$ is given by the number of states with $M_{\text{Tot}} = M - 1$, i.e.,

$$D(M) = D_{\text{Tot}}(M) - D_{\text{Tot}}(M - 1) = P_N(M) - P_N(M - 1), \quad (29)$$

with $P_N(-1) \equiv 0$.

Figure 7 shows the degeneracy of the lowest Landau level for three identical bosons as a function of internal angular momentum M . Several interesting things emerge in this figure. First, we can see that, as stated above, there are no allowed bosonic states with internal angular momentum $M = 1$. This is because there is only one lowest Landau level state with total angular momentum $M_{\text{Tot}} = 1$ when $m_1 = 0$, $m_2 = 0$, and $m_3 = 1$ where m_i is defined as in Eq. (28). Since we know there is a bosonic state with internal angular momentum $M = 0$, the only way to get total angular momentum $M_{\text{Tot}} = 1$ is then with $M = 0$ and $M_{\text{c.m.}} = 1$.

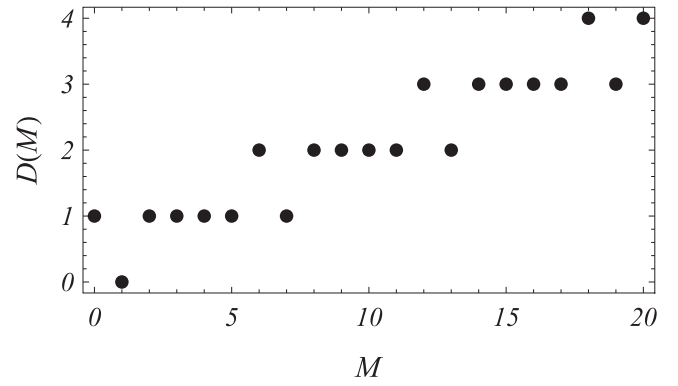


FIG. 7. The degeneracy of the lowest Landau level for three identical bosons is shown as a function of internal angular momentum M . Note that for $M = 6n$ where $n = 1, 2, 3, \dots$, there is an anomalously high level of degeneracy.

We can also observe in Fig. 7 that for $M = 6n$, $n = 1, 2, 3, \dots$, the lowest Landau level presents an unusually high level of degeneracy where the degeneracy is higher than both that of $M + 1$ and $M - 1$. We note that these anomalously high-degeneracy values of M correspond exactly to the angular momentum of the three-boson Laughlin states [2] whose wave functions are given by

$$\Psi_L(z_1, z_2, z_3) = \mathcal{N} e^{(-\sum_j |z_j|^2/l_c^2)} \left[\prod_{i < j} (z_i - z_j)^{2n} \right], \quad (30)$$

where \mathcal{N} is again a normalization constant and $n = 1, 2, 3, \dots$. These states are lowest Landau level states in which each particle pair has an interparticle angular momentum of $2n$ giving a total angular momentum of $M_{\text{Tot}} = N(N - 1)n = 6n$ for $N = 3$. Because the prefactor in Eq. (30) only depends of the position of the particles relative to each other, it contains no center-of-mass angular momentum $M_{\text{c.m.}} = 0$. We also note that the same degeneracy pattern as seen in Fig. 7 for three bosons occurs for three identical fermions, but shifted to the right by $M = 3$ (the minimum allowed angular momentum for three fermions in the lowest Landau level).

As discussed above, when the lowest Landau level becomes degenerate, for $M = 6$ and $M \geq 8$ here, there exists at least one state in which each particle pair has no zero angular momentum component, and which consequently do not experience the s -wave pseudopotential. This means that, for weakly repulsive interactions, $a \ll l_c$, the lowest-energy three-body states are noninteracting lowest Landau level states with $E = \hbar\omega_c$ for these values of M .

If a repulsive d -wave interaction were to be included in this system, any state with an $m = 2$ component in its interparticle angular momentum would experience the interaction. We can assume that the d -wave interaction would generally have a smaller effect on these states than the s -wave interaction has on states with an $m = 0$ interparticle angular momentum component. However, we surmise that the pattern of the energy shift from the lowest Landau level would be similar for these d -wave interacting states to the s -wave interacting states, mainly the pattern of even-odd parity oscillation. Further, when the degeneracy jumps up to three degenerate states or more (for

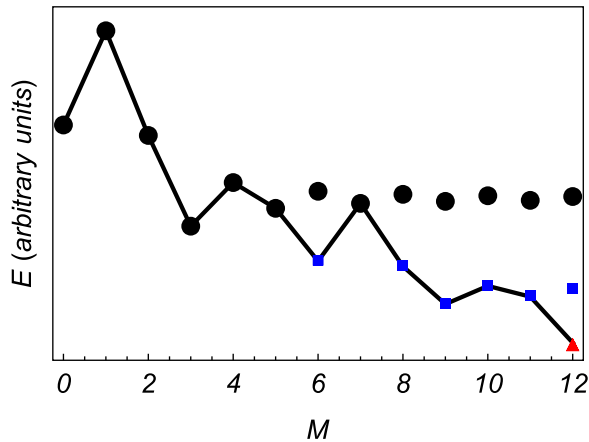


FIG. 8. A schematic illustration of the possible energy structure of the three-boson system is shown as a function of internal angular momentum M . This schematic illustrates the possible interplay between even-odd parity oscillations in the energy and the degeneracy pattern which could result in ground-state energies that reflect a “magic number” type behavior.

$M = 12$ and $M \geq 14$) there will exist states with only $m \geq 4$ interparticle angular momentum components. These higher angular momentum states will not experience either the s - or d -wave interactions.

Figure 8 shows a schematic representation of the energies that might result from including a repulsive d -wave interaction. We emphasize here that the energies shown here are purely schematic in nature and are shown only to illustrate the surmised structure of the lowest-energy states for weakly repulsive interactions. Here, black circles represent the energies of states which are experiencing the s -wave interaction, while blue squares represent states which only experience a d -wave interaction. A single red triangle at $M = 12$ represents a state with no s - or d -wave interparticle angular momentum [this is in fact the Laughlin state of Eq. (30) with $n = 2$]. The even-odd oscillation combined with the pattern of degeneracies for three identical bosons creates an interesting overall pattern of lowest-energy states (marked in Fig. 8 by the solid line) in which the ground-state energy for each value of M tends to decrease overall with increasing M . However, every third state, $M = 0, 3, 6, 9,$ and 12 here, is lower in energy than either of its neighbors. This pattern of anomalously low-energy states is similar to the “magic number” states first predicted in Ref. [8] for fermions interacting via the repulsive Coulomb interaction. It is possible then that the appearance of the magic numbers for three-particle systems with repulsive interactions is simply a manifestation of the combination of even-odd oscillations in

the energy with the pattern of degeneracy for three identical particles.

VI. SUMMARY

The three-boson problem in 2D in the presence of a transverse magnetic field is surprisingly well described using the adiabatic hyperspherical method. The full energy spectrum presents very narrow avoided crossings between the adiabatic energies, and away from these crossings the couplings between channels can be largely ignored to a good approximation. This indicates that the system is nearly separable in the hyperspherical picture. The adiabatic hyperspherical picture provides a useful interpretation of transitions in which excitations between levels can be achieved through either a hyperangular excitation in which the internal configuration of the three-boson system is changed or through a hyperradial vibrational excitation in which the internal structure of the system remains the same. The adiabatic hyperangular eigenvalues $\varepsilon_{nM}(R)$ are exactly the same as those found for three interacting bosons in free space. The inclusion of the magnetic field results in the addition of an effective isotropic trap, and an angular-momentum-dependent shift.

When interacting via the s -wave pseudopotential, three-body states transition from the weakly repulsive regime ($a \ll l_c$) to the weakly attractive regime ($a \gg l_c$) as a function of the 2D scattering length. States that interact via the s -wave interaction display an even-odd parity oscillation as a function of the total internal angular momentum M . For small scattering length, this parity oscillation combined with the fact that there is no $M = 1$ lowest Landau level means that the lowest interacting three-boson state has total internal angular momentum $M = 3$. At higher values of angular momentum the lowest Landau level becomes degenerate and a set of noninteracting states emerge in which the inter-particle angular momentum has no $m = 0$ component. Interestingly, if the same pattern of even-odd parity oscillations persists when higher partial wave interactions are included, in combination with the pattern of degeneracy for the lowest Landau level, this might be the source of the “magic number” behavior seen in three-particle systems interacting via long-range Coulomb interactions, and is the subject of ongoing work.

ACKNOWLEDGMENTS

The authors would like to thank B. M. Peden, D. Blume, and J. P. D’Incao for helpful discussions and insights. S.T.R. acknowledges support from NSF Grants No. PHY-1516337 and No. PHY-1516421 and from a Cottrell College Science Award through the Research Corporation for Scientific Advancement.

- [1] D. C. Tsui, H. L. Stormer, and A. C. Gossard, *Phys. Rev. Lett.* **48**, 1559 (1982).
- [2] R. B. Laughlin, *Phys. Rev. Lett.* **50**, 1395 (1983).
- [3] B. Yang, *Phys. Rev. B* **87**, 245132 (2013).
- [4] Y.-L. Wu, B. Estienne, N. Regnault, and B. A. Bernevig, *Phys. Rev. B* **92**, 045109 (2015).
- [5] F. Wilczek, *Phys. Rev. Lett.* **48**, 1144 (1982).

- [6] F. Wilczek, *Phys. Rev. Lett.* **49**, 957 (1982).
- [7] J. K. Jain, *Phys. Rev. Lett.* **63**, 199 (1989).
- [8] S. M. Girvin and T. Jach, *Phys. Rev. B* **28**, 4506 (1983).
- [9] W. Lai, K. Yu, Z. Su, and L. Yu, *Solid State Commun.* **52**, 339 (1984).
- [10] M. Stone, H. W. Wyld, and R. L. Schult, *Phys. Rev. B* **45**, 14156 (1992).

- [11] B. L. Johnson and G. Kirczenow, *Phys. Rev. B* **47**, 10563 (1993).
[12] G. Moore and N. Read, *Nucl. Phys. B* **360**, 362 (1991).
[13] V. Gurari and C. Nayak, *Nucl. Phys. B* **506**, 685 (1997).
[14] P. Bonderson, V. Gurarie, and C. Nayak, *Phys. Rev. B* **83**, 075303 (2011).
[15] B. L. Johnson and S. A. Langer, *Phys. Rev. B* **49**, 7511 (1994).
[16] K. S. Fine, A. C. Cass, W. G. Flynn, and C. F. Driscoll, *Phys. Rev. Lett.* **75**, 3277 (1995).
[17] B. L. Johnson and J. A. Hayes, *Phys. Rev. B* **63**, 235312 (2001).
[18] Y. F. Ge, *Europhys. Lett.* **16**, 11 (1991).
[19] B. L. Johnson and G. Kirczenow, *Rep. Prog. Phys.* **60**, 889 (1997).
[20] R. B. Laughlin, *Phys. Rev. B* **27**, 3383 (1983).
[21] K. M. Daily, R. E. Wooten, and C. H. Greene, *Phys. Rev. B* **92**, 125427 (2015).
[22] L. M. Delves, *Nucl. Phys.* **9**, 391 (1959).
[23] L. M. Delves, *Nucl. Phys.* **20**, 275 (1960).
[24] Y. F. Smirnov and K. V. Shitikova, *Fiz. Elem. Chastits Yadra* **8**, 847 (1977) [*Sov. J. Nucl.* **8**, 344 (1977)].
[25] J. S. Avery, *Hyperspherical Harmonics: Applications in Quantum Theory* (Kluwer Academic, Norwell, MA, 1989).
[26] J. S. Avery, *J. Phys. Chem.* **97**, 2406 (1993).
[27] S. T. Rittenhouse, M. J. Cavagnero, J. von Stecher, and C. H. Greene, *Phys. Rev. A* **74**, 053624 (2006).
[28] E. Nielsen, D. V. Fedorov, and A. S. Jensen, *Phys. Rev. A* **56**, 3287 (1997).
[29] E. Nielsen, D. V. Fedorov, A. S. Jensen, and E. Garrido, *Phys. Rep.* **347**, 373 (2001).
[30] D. S. Petrov, M. Holzmann, and G. V. Shlyapnikov, *Phys. Rev. Lett.* **84**, 2551 (2000).
[31] A. S. Jensen, K. Riisager, D. V. Fedorov, and E. Garrido, *Rev. Mod. Phys.* **76**, 215 (2004).
[32] O. I. Kartavtsev and A. V. Malykh, *Phys. Rev. A* **74**, 042506 (2006).
[33] J. P. D’Incao and B. D. Esry, *Phys. Rev. A* **90**, 042707 (2014).
[34] E. Nielsen, D. V. Fedorov, and A. S. Jensen, *Few-Body Syst.* **27**, 15 (1999).
[35] H.-W. Hammer and D. T. Son, *Phys. Rev. Lett.* **93**, 250408 (2004).
[36] K. Kanjilal and D. Blume, *Phys. Rev. A* **73**, 060701 (2006).
[37] S.-M. Shih and D.-W. Wang, *Phys. Rev. A* **79**, 065603 (2009).
[38] S. T. Rittenhouse, N. P. Mehta, and C. H. Greene, *Phys. Rev. A* **82**, 022706 (2010).
[39] K. Helfrich and H.-W. Hammer, *Phys. Rev. A* **83**, 052703 (2011).